The combination of bacterial polymer and tragacanth to form antimicrobial biofilter for desalination

Zarrindokht Emami[a], Giti Emtiazi[a,*], Iraj Nahvi[a], Alimohammad Ahadi[b], Mohammad Hossein Hashemol-Hosseini[c]

[a]*Department of Biology, Faculty of Sciences, University of Isfahan, Isfahan, Iran, emails: zarrrindokht20@gmail.com (Z. Emami), emtiazi@yahoo.com, emtiazi@sci.ui.ac.ir (G. Emtiazi), i.nahvi@sci.ui.ac.ir (I. Nahvi)*
[b]*Department of Genetic, Faculty of Science, University of Sharekord, Shahr-e Kord, Iran, email: ahadi52@gmail.com*
[c]*Process Engineering and Planning, Esfahan Oil Refining Company, Isfahan, Iran, email: hashemolhossaini@eorc.ir*

a b s t r a c t

Different polymers including tragacanth, vermiculite, perlite, silica gel and bacterial polymer were used to form biofilter for desalination. Salt tolerant Z1 bacterium was isolated from leachate and identified as *Bacillus atrophaeus.* It could produce high amount of exopolysaccharide with antifungal activity. The biofilters were made to contain several layers that include a thin layer of cotton, silica gel, tragacanth itself or tragacanth plus Z1 or Z1 exopolysaccharide, vermiculite and perlite. The biofilter included tragacanth itself had the capability to remove ammonium by 5% from 1 mM solution of NH_4Cl. Adding Z1 bacterium to tragacanth, ammonium removal increased to 72%. Different salt solutions were exposed to certain amounts of alive Z1 bacterium, boiled Z1 bacterium and Z1 polysaccharide. Among them, extracted Z1 exopolysaccharide showed the most efficiently on the desalination of iron and cupper by 84.93% and 89.74%, respectively. Therefore, a synergistic effect of mixed Z1 exopolysaccharide with antifungal activity and tragacanth, to make biofilter were studied to remove different ions from salted well water. Our results have indicated that using Z1 polysaccharide and tragacanth in biofilter construction could effectively reduce Ca, Cl, Na, K, Pb, Cd and Zn from brackish well water. Using Z1 polysaccharide instead of Z1 bacterium prevents biofouling in biofilter construction. The different tests include UV-Vis spectroscopy, Fourier transform infrared spectroscopy (FTIR), X-ray diffraction and atomic absorption were used for relatively understanding the performed processes. FTIR analysis of Z1 polysaccharide itself, and with different salts showed interaction of Z1 polysaccharide functional groups, such as –OH, –COO and C–O–C involved in different ions and metal biosorption process.

Keywords: Antimicrobial biofilter; *Bacillus atrophaeus;* Bacterial polymers; Microbial desalination; Tragacanth

1. Introduction

The water crisis is one of the oldest and most important problems in the world. With increasing population and decreasing freshwater sources, using different desalination methods to reduce salt from brackish or saline water, and re-use wastewater and remove salts from available sources is considered as an important strategy for solving this problem. For this manner, several treatment methods, such as chemical precipitation, membrane filtration, reverse osmosis, ion exchange, and adsorption have been used for the removal of different salts, heavy metals and dyes [1–6]. Among them, adsorption is known as the preferable methods for wastewater treatment. It could be due to its potential to absorption different materials and its simplicity of design [7,8]. Many natural and synthetic polymers such as silica gel, vermiculite, perlite and tragacanth could be used as adsorbents in

* Corresponding author.

absorption method. Silica gel is a granular, porous form of silicon dioxide made synthetically from sodium silicate. It is a naturally occurring mineral that is purified and processed into either granular or beaded form. It has a strong affinity for water molecules; therefore, it is used as a desiccant to control local humidity to avoid spoilage or degradation of some materials. It could be simultaneous adsorption of cations and anions from aqueous solution [9]. Vermiculite and perlite are porous ceramics. Vermiculite is a hydrous phyllosilicate mineral by a high cation exchange capacity [10]. Perlite is an amorphous volcanic glass with high water content, typically formed by the hydration of obsidian. It is an industrial mineral and a commercial product useful for its light weight after processing [11]. Tragacanth is a natural gum obtained from the stems and branches of *Asiatic* species of *Astragalus* [12,13]. Gum tragacanth (GT) is a branched, heterogeneous, anionic carbohydrate consists of a linear 1, 4 linked α-D-galacturonic acid backbone with three types of side chains: single β-D-xylopyranose and disaccharide units of 2-O-α-L-fucopyranosyl-D-xylopyranose and 2-O-β-D-galactopyranosyl-D-xylopyranose [14]. GT is one of the most acid resistance gums having two major structures: tragacanthin, water-soluble part of tragacanth make of galacturonic acid, and bassorin that is insoluble in water and water-swellable. It was shown that tragacanth have antimicrobial activity against fungi and different gram-negative and gram-positive bacteria [15]. Presumably the L-sugars constitute of tragacanth (L-arabinose and L-fucose) are responsible for its antimicrobial activity and resistance to microbial biodegradation. Usually most organism would not be able to metabolize these kinds of sugars [16].

Biosorption is an alternative method of adsorption and referred to such treatment methods that employs a wide variety of biological agents such as algae, fungi, and bacteria [17]. It could employ non-living biomass such as killed microorganisms, exopolysaccharides or other polymers produced by living cells. It was shown that pretreatment and killing of biomass either by physical or by chemical treatment or crosslinking could be improved the biosorption capacity of biomass [18]. *Bacillus* is a genus of gram-positive, rod-shaped spore forming bacteria and a member of the phylum Firmicutes. Some species could be produced exopolysaccharide to form capsule. They could be reacting as absorbent in wastewater treatment [17,19–23]. The aim of this study was to investigate desalination of NH_4Cl, $NaCl$, $FeCl_3$, $CuSO_4$, Na_2SeO_3 and $CoCl_2$ by a variety of natural and synthetic polymers such as tragacanth, silica gel, vermiculite and perlite, and a *Bacillus* species isolated from leachate. The different tests like UV-Vis spectroscopy, Fourier transform infrared spectroscopy (FTIR) and X-ray diffraction (XRD) and atomic absorption were used for relatively understanding the performed processes.

2. Materials and methods

2.1. Isolation of salt tolerant Bacillus *from leachate*

The salt tolerant *Bacillus* strain for microbial desalination was isolated from municipal leachate. Heat shocking at 80°C for 10 min was done to obtain spore suspension. Serial dilution of samples were prepared and the 0.1 ml of them were cultured on Caso Agar medium supplemented by 15% NaCl by pour plate technique. Plates were incubated aerobically at 28°C for 24 h for the growth of the genus *Bacillus* as the aerobic spore-forming microorganisms. The pure culture of each isolated strains were obtained on Caso Agar. Among them, Z1 strain was selected for further studies because of producing large quantities of exopolysaccharides based on its mucoidal colony. The pure culture was maintained on Caso Agar slants and stored at 4°C.

2.2. Identification of bacterial strain

Z1 strain showed the maximum salt tolerance and exopolysaccharide production identified by morphological and molecular characteristics. Molecular identification of the strain was performed by 16S rDNA sequencing. The genomic DNA was extracted by the boiling method according to the procedure described by Zhou and Jiao [24]. Universal primers RW01 (5′-ACCTGGAGGAAGGTGGGGAT-3′) and DG74 (5′-AGGAGGTGATCCAACCCGCA-3′) were used for amplification of the 16S rDNA gene for a ribo-typing procedure using the EzTaxon server (http://www.ezbiocloud.net/eztaxon [25]). The results were analyzed and compared by using the BLAST server (http://www.ncbi.nlm.nih.gov/BLAST), and finally, the phylogenetic tree was constructed using the MEGA6.0 program [26].

2.3. Exopolysaccharide extraction

Z1 strain was cultured on Caso Agar medium for 24 h at 30°C. Harvested bacterial suspension in distilled water was centrifuged at $447 \times g$ for 5 min to remove bacterial cell. Two volumes of cold ethanol in 96% were added to supernatant and kept at –20°C for 24 h to precipitate the polysaccharides. The suspension was centrifuged at $7155 \times g$ for 1 h. Additional alcohol was removed from the tube, and the whole precipitated polysaccharide was dried at room temperature.

Extracted exopolysaccharide construction was examined by several methods. Concentration of polysaccharide in extracted polymer was estimated by anthrone assay against glucoses standard curve as described by Gholampoor et al. [27]. The total protein in extracted polymer was determined using Bradford assay against bovine serum albumin standard curve. FTIR analysis was used for identification of functional groups of extracted polymer.

2.4. Antifungal activity of Z1 and Z1 polysaccharide

One of the problems in biofilter construction is biofouling mostly caused by fungal pollution. The antifungal properties of Z1 and Z1 polysaccharide were studied against fungal pollutions on PDA medium. Certain amounts of precipitated Z1 bacterium in nutrient broth (NB) and Z1 polysaccharide were placed on sterile blank disks. Common biofilter fungal pollutions, which observed in biofilters stored in the laboratory and refrigerator, were placed against them. Antifungal properties were detected after 7 d.

2.5. Biofilter construction

One of the most common methods for desalination studies is using biofilter. In this study, several biofilters was

constructed in 5 ml sterile syringes. Each filter contained 1 g of silica gel on a little amount of cotton, which was filled by a layer containing 3 g of 20% (w/v) tragacanth plus different kind of bacterial or biological polymers. A schematic view of these filters is shown in Fig. 1.

2.6. Effect of biofilters on NH_4Cl removal

After preparation of each filter, 5 ml of 1 mM solution of NH_4Cl in phosphate buffer (pH = 7) was filtrated by pushing the syringe slowly to pass the whole solution after 5 min. The amount of NH_4Cl in filtrate was measured by Nessler method [28]. The absorbance of yellow to orange color produced by the Nessler-ammonia reaction was measured at 410 nm. The concentration of remained NH_4Cl in each sample was determined via standard curve of NH_4Cl.

2.7. XRD analysis

XRD analysis of the Z1 polysaccharide was performed by X-ray diffractometer, D8ADVANCE (Bruker, Germany). X-rays were produced by a copper X-ray tube with wavelength 1.5406 A (Cu Kα) and Ni as a filter. Measurements were performed between 10° and 90° 2θ.

2.8. UV-Vis spectra analysis for other salts removal

Removal of different salts by alive Z1 bacterium, Z1 on Caso Agar, sterile Caso Agar alone, boiled Z1 bacterium and Z1 polysaccharide were examined by adding the certain amounts of them to different salt solutions: Fe_2O_3 0.005%, NH_4Cl 1 mM, $FeCl_3$ 0.5%, $CuSO_4$ 1.5%, NaCl 0.9%, $CoCl_2$ 1%, $K_2Cr_2O_7$ 0.2%, $NiCl_2$ 2% and Na_2SeO_3 1 mM. After 3 d, measurments were performed by measuring the optical density of the samples in the wavelengths ranging from 200 to 800 nm by UV-Visible spectrophotometer (Shimadzu UV-160, Japan). The best samples were selected for further studies.

2.9. FTIR analysis

The dried exopolysaccharide were added to 25 ml of distilled water and several salt solutions. After 3 d, suspensions were centrifuged separately, and the pellets were rinsed by deionized water completely and dried in the oven with temperature 50°C. The structure were analyzed by the FTIR technique (6300 model, JASCO, Japan) to determined functional groups , in the range 4,000–400 cm^{-1} at a resolution of 4 cm^{-1} by making the KBr thin pellet. The results were analyzed by IRPal software.

2.10. The effect of bacterial polymers and tragacanth on different ions removal

The 30 ml of well water that include different elements and ions were passed from tragacanth or tragacanth with Z1 polysaccharide separately. In each filters, 1 g tragacanth were added to 5 ml distilled water or 5 ml of 20% (w/v) Z1 polysaccharide solution. The concentrations of Ca, K, Ni, Pb, Cd and Zn in the both well water and filtrates were analyzed by atomic absorption spectrophotometry (Model 3030, PerkinElmer, USA).

3. Results and discussion

3.1. Bacterial identification

Our results demonstrated that Z1 strain, which showed the maximum salt tolerance and exopolysaccharide production, is a gram-positive spore forming bacteria with mucoidal colonies on Caso Agar. DNA extraction and PCR by universal primers were performed, and the 370 bp amplicons were analyzed. The bacterial isolates were identified using the EzTaxon server (http://www.ezbiocloud.net/eztaxon [25]) on the basis of 16S rRNA sequence data. Comparing the sequences by using BLAST server showed the most related species as *Bacillus atrophaeus* with a 97.87% similarity. Phylogenetic and molecular evolutionary analyses were conducted using MEGA version 6 [26]. Neighbor-joining phylogenetic tree based on provided 16S rRNA gene sequences showed the position of strain Z1 among the related species in Bacillaceae family (Fig. 2) with submission numbers SUB1222599.

Bacillus atrophaeus is a gram-positive, aerobic, spore forming bacteria phenotypically similar to *B. subtilis*, except for the production of a pigment when cultured in media containing an organic nitrogen source [29]. *B. atrophaeus* has a wide variety of biotechnological applications. Sella et al. [30] studied the taxonomy, multicellularity, life cycle, and some aspects of biotechnological applications of *Bacillus atrophaeus* as a biomolecule producer. They showed that *Bacillus atrophaeus* could be a vehicle and adjuvant for vaccine and as a biological indicators to evaluate the efficiency of the sterilization processes. The use of *Bacillus atrophaeus* in astrobiology and biodefense studies and as a biocontrol and plant growth promoting agent was demonstrated by them. They believed that due to their safety, high resistance, high production and cost effectiveness, *Bacillus atrophaeus* is a highly attractive microorganisms for biotechnological applications [30].

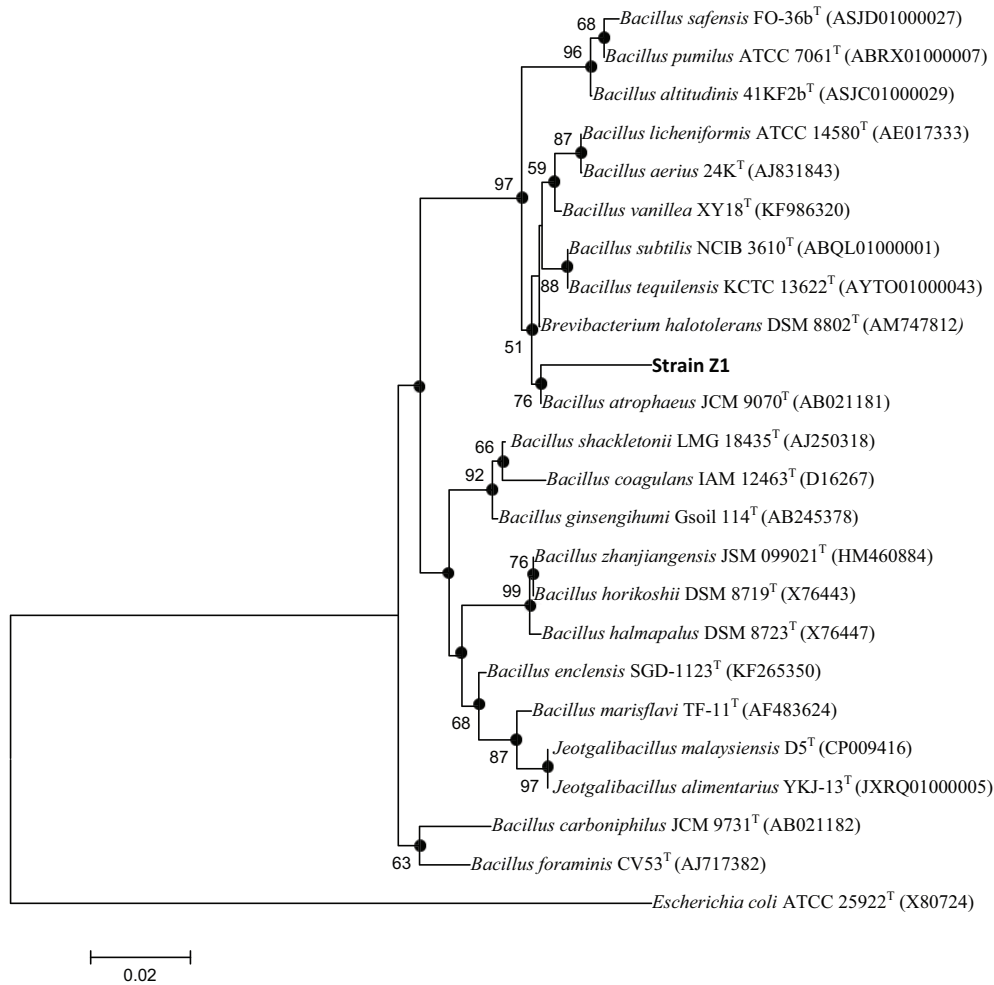Fig. 1. Schematic view of biofilter construction.

Fig. 2. Phylogenetic tree of Z1 strain. Bold nodes indicate branches that were also obtained by minimum-evolution and maximum-like-lihood methods. Numbers at nodes indicate levels of bootstrap support (%) based on analysis of 1,000 resembled datasets; only values above 50% are given. Bar, 0.02 substitutions per nucleotide position. The sequence of Escherichia coli ATCC 25922T was used as out-group.

3.2. Exopolysaccharide construction

Extracted Z1 exopolysaccharide construction was examined by different methods. Concentration of polysaccharide in extracted polymer was estimated by anthrone assay against glucoses standard curve as 1.72 mg/L. The amount of protein in extracted polymer was determined by Bradford assay against bovine serum albumin standard curve as 5.236×10^{-3} mg/l. Due to these results, it was shown that the most constitute of exopolymer as 99.69% was polysaccharide. FTIR analysis was used for identification of functional groups of extracted exopolysaccharide (Fig. 3).

Several studies were performed about using FTIR in analysis of foodborne pathogenic bacteria [31]. It could be used for detection and quantification of bacteria from culture and food, discrimination of viable, injured and dead bacteria, taxonomic classification of bacteria and analysis of structural components of bacteria [31]. In this study, we used FTIR for studying functional groups of Z1 polysaccharide. According to a simple approach to analysis of
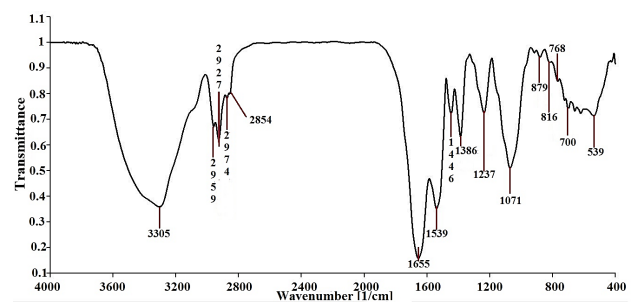
Fig. 3. FTIR spectrum of Z1 strain exopolysaccharide.

FTIR spectrum, looking a strong absorption in the region 1,655 cm^{-1} (1,820–1,660 cm^{-1}) showed that there is a carbonyl group (C=O) in the polysaccharide. Presence of a broad band near 3,400–2,400 cm^{-1} (3,305 cm^{-1}) showed that it is carboxylic acids (–COOH) bond in the polysaccharide. Two weak absorptions near 2,870 and 2,750 cm^{-1} (2,875

and 2,854 cm^{-1}) indicated aldehyde group (H–C=O) in polysaccharide construction. Aromatic C–H occurs to the left of 3,000 cm^{-1} and aliphatic C–H occurs to the right of 3,000 cm^{-1}. Two absorptions at 2,959 cm^{-1} (2,965–2,955 cm^{-1}) and 2,927 cm^{-1} (2,930–2,920 cm^{-1}) indicated –CH$_3$ and –CH$_2$–, respectively. There are two absorptions at 1,600–1,530 cm^{-1} (1,539 cm^{-1}) and 1,390–300 cm^{-1} (1,386 cm^{-1}) that indicated nitro groups in the polymer structure. Medium bound at 1,446 cm^{-1} (1,500–1,400 cm^{-1}) indicated C–C in ring of aromatics. Medium bound at 1,237 cm^{-1} and strong bound at 1,071 cm^{-1} (1,320–1,000 cm^{-1}), both of them reconfirmed C–O stretch bound in carboxylic acid. Strong band at 1,071 cm^{-1} can be assigned C–C stretching in the pyranoid ring [32]. Presence of absorption at fingerprint regions (879 cm^{-1} (885–870 cm^{-1}: 1,2,4-trisubstituted), 816 cm^{-1} (825–805 cm^{-1}: 1,2,4-trisubstituted), 768 cm^{-1} (780–760 cm^{-1}: 1,2,4-trisubstituted) and 700 cm^{-1} (710–690 cm^{-1}: monosubstituted) indicated C–H out of plane bonds in aromatic compound structure of polysaccharide (Table 1). There is a 539-cm^{-1} bond (689–500 cm^{-1}) in the spectrum that it could be indicated C–Br in the structure.

3.3. Antifungal properties of Z1 bacterium and Z1 polysaccharide

Tragacanth gum (TG) is a biodegradable polymer with good properties. The physical, chemical and biological properties of TG including structure, thermal behavior, emulsifying, viscosity, acidity, stability, and also rheological, antibacterial, antifungal, biocompatibility and biodegradability have been reported by various researchers [15,33–37]. The main structure of our biofilters was tragacanth. Our biofilters polluted by some fungi after long time. We wanted to increase antifungal activity of tragacanth gum by adding Z1 bacterium. *Bacillus atrophaeus* produced surfactin, which is a biosurfactant. Biosurfactants are proteins that showed antimicrobial, emulsifier and detergent activities [38]. It was

shown that *Bacillus atrophaeus* could produce bacteriocin, which showed antimicrobial and antifungal activities [39]. Antifungal activities of *Bacillus atrophaeus* against various fungal pathogens of cucumber and tomato have been suggested by Zhang et al. They indicated that all extracted compounds include lipopeptides, secreted proteins and volatile compounds produced by this strain involved in its antifungal activities [40]. But biofouling may accrued by adding Z1 strain to biofilter [41]. Therefore, we decided to use Z1 biomaterials with antimicrobial activity. Among them, proteins and polypeptides may be denatured under undesirable conditions, and polysaccharide extraction is easier and more cost effective than proteins and polypeptides extraction; therefore, we decided to examine antifungal activities of Z1 polysaccharides for adding it to biofilter construction. In this research, both Z1 bacterium and Z1 polysaccharide showed antifungal activity. As it was shown at Fig. 4, Z1 bacterium had more antifungal activity than Z1 polysaccharide. It could be due to other antifungal materials, such as the bacteriocin subtilosin [42] with antimicrobial activity and lypolytic properties [39] or bioactive compounds such as bacillamide C and neobacillamide A [43], or biosurfactant proteins with emulsifiers, detergents and antimicrobial activities [38].

3.4. Effect of biofilters on NH$_4$Cl removal

Several filters were prepared by tragacanth and different kinds of bacterial and chemical compounds (Fig. 5). In the all experiments, 5 ml of 1 mM solution of NH$_4$Cl was filtrated at the time zero. Initially, NH$_4$Cl removal by different part of each biofilters checked to determine the best parts for using them in biofilter construction. In our experiments, we used silica gel to maintain tragacanth and its derivatives in biofilter. It was shown that silica gel had no effect on ammonium removal; therefore, we considered to test other materials to replace it. Vermiculite and perlite

Table 1
Definition of FTIR bonds selected from IRPal software

| Polysaccharide	Class	Structure	High–Low	Typical second	Intensity	Assignment
3,305	Carboxylic acids	RCO–OH	3,400–2,800		S (broad)	Dimer OH
2,959	Alkanes	–CH$_3$	2,965–2,955	2,960	M, S	–CH$_3$
2,927	Alkanes	–CH$_2$–	2,930–2,920	2,925	M, S	–CH$_2$–
2,874	Alkanes	–CH$_3$	2,875–2,865	2,870	M, S	–CH$_3$
2,854	Alkanes	–CH$_2$–	2,855–2,845	2,850	M, S	–CH$_2$–
1,655	Amides	RCONH´R	1,655–1,645	1,650	S	C=O stretch (H-bond)
1,539	Misc.	N–O nitro comp	1,545–1,535	1,540–1,380	S	N–O asym. strech
1,446	Aromatics	C–C in ring	1,500–1,400		M	Ar C–C stretch
1,386	Misc.	S=O sulfate	1,450–1,350		S	S=O sulfate ester
1,237	Carboxylic acids	RCO–OH	1,300–1,150		M	C–O stretch
1,071	Carboxylic acids	RCO–OH	1,320–1,000		S	C–O stretch
879	Aromatics	1,2,4-trisub.	885–870	877	M	C–H out of plane
816	Aromatics	1,2,4-trisub.	825–805	815	M	C–H out of plane
768	Aromatics	1,2,4-trisub.	780–760	770	M	C–H out of plane
700	Aromatics	Monosubst.	710–690	700	M	C–H out of plan
536	Alkyl halides	R–Br	689–500		S	C–Br stretch
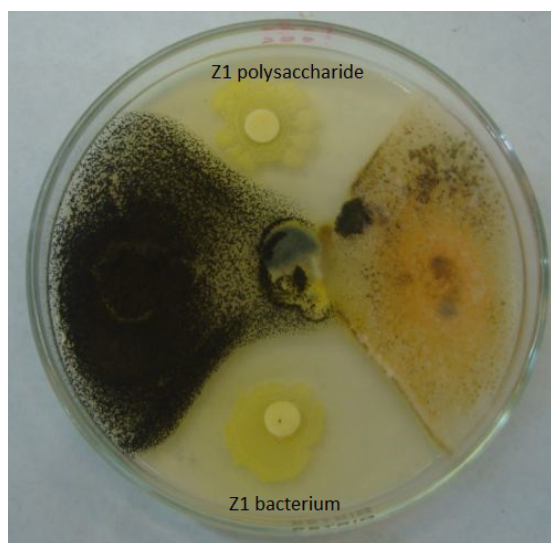
Fig. 4. Antifungal activity of Z1 bacterium and Z1 polysaccharide.
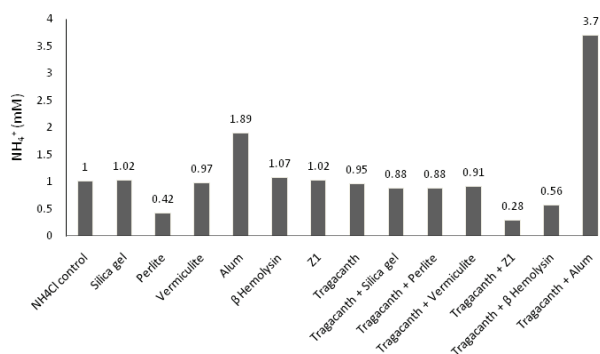

Fig. 5. Different biofilter construction.

Fig. 6. Concentration of NH_4^+ (mM) remained in different filtrate.

were used for this manner, like silica gel; they had no significant effect on the content of ammonium in the effluent, but they were the more cost effective. Vermiculite was used for the first layer in biofilters. Among different biofilters, tragacanth with Z1 bacterium showed the most effect on ammonium removal (Fig. 6). The reminded ammonium in filtrate was 0.28 mM. This kind of biofilter could remove 72% of ammonium from initial influent. Surprisingly, tragacanth itself and Z1 itself had no significant effect on removal of ammonia, but together they had synergistic effect on ammonium removal.

Treating of silica gel with different reactive groups could be prepared selective adsorbent [44]. Wang et al. [9] treated silica gel by adding a ditopic zwitterionic Schiff base to simultaneous adsorption of anions and cations from aqueous solutions. Chemically activated vermiculite by H_2O_2 or HCl affected the removal efficiency for both cadmium and lead ions [10]. The initial concentration and triangular molecular structure of methylene blue (MB) and crystal violet (CV) affected the adsorption behavior of them onto natural vermiculite [45]. The in vitro binding capacity of eight non-starch polysaccharides such as tragacanth gum to zinc, iron and calcium showed that except iron, there were no significant binding in acidic condition, but in natural condition, the amount of binding affected by cation exchange capacity of the polysaccharide [36]. Natural polysaccharide-based interpenetrating polymer network (IPN) such as tragacanth could adsorb crude oil from water due to its high affinity for it [13]. Combination of silica gel, vermiculite, tragacanth and Z1 bacterium as a strain of *Bacillus atrophaeus* in our biofilters construction increased different salt removal capacity by them.

3.5. The effect of Z1 polysaccharide on NaCl sorption detected by XRD analysis

XRD analysis of Z1 polysaccharide showed that this polymer absorbed NaCl from its environment, and they were coupling together tightly and reminded with its structure even after washing them. The XRD patterns of the polysaccharide samples precipitated in alcohol are shown in Fig. 7. Several reflections were observed in the region 5° < 2θ < 80° for the patterns of them. This pattern is defined as Halite that its formula is NaCl. This indicate that Z1 polysaccharide could absorbed NaCl from its environment (Fig. 7). Some functional groups such as carbonyl group in carboxylate anionic form can be the cause of Na^+ absorption by Z1 polysaccharide. Strong peak at 1,655 cm^{-1} in FTIR spectra can be assigned to carbonyl group in carboxylate anionic form (COO$^-$) [32] confirmed that Z1 polysaccharide could adsorbed Na^+ [46] by this functional group.

3.6. UV-Vis spectra analysis results for different ions removal

By these experiments, it was found that Z1 bacterium showed significant effect in microbial desalination.

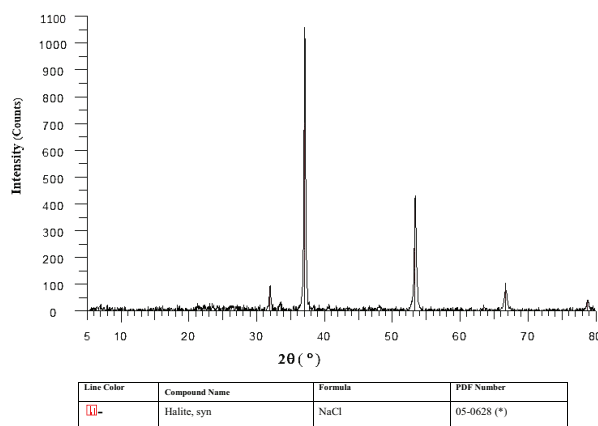| Line Color	Compound Name	Formula	PDF Number
—	Halite, syn	NaCl	05-0628 (*)

Fig. 7. XRD analysis of polysaccharide precipitated in alcohol.

For further studies, several topics should be noticed: (a) which part of the bacterium had more effect on desalination, and (b) if there were any differences between the kinds of salt and its desalination. Therefore, certain amounts of alive Z1 bacterium, boiled Z1 bacterium and Z1 polysaccharide were added to different salt solutions. $FeCl_3$ as an example sample is shown in Fig. 8.

The effect of the samples on different salt solutions were checked by measuring the optical density of the samples in the wavelengths ranging from 200 to 800 nm by UV-Visible spectrophotometer. The results showed that Z1 polysaccharide had the most potential in the microbial desalination. Colored salts such as $CuSO_4$, $FeCl_3$, $CoCl_2$ and Na_2SeO_3 had detectable peaks in certain wavelengths. But there was no significant peak for colorless salts such as NH_4Cl. Reminded NH_4^+ in this cases were measured by adding Nessler reagent. In order to study desalination, the absorption in the same peaks of the control and sample curves were compared together (Fig. 9). Reduce the absorption in the specific wavelength indicates the removal of salt by a sample that is shown as the salt removal percentage. The results are shown in Table 2.

The results showed that Z1 polysaccharide had the most effect on $CuSO_4$ desalination (89.74% at 415 nm). After that, $FeCl_3$ and NH_4Cl were removed significantly by Z1 polysaccharide. There were no considerable effects in other salts. For further studies, FTIR analysis was performed on the pellet of the polysaccharide in each solution after rinsing and drying them.

Fig. 8. Effect of Z1 and Z1 polysaccharide on removal of $FeCl_3$ 0.5%.
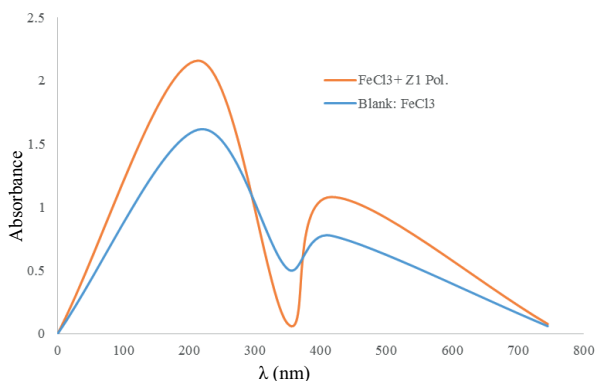
Fig. 9. Comparison of the absorbance in the peaks of UV-Visible spectra in $FeCl_3$ and $FeCl_3$ with Z1 polysaccharide.

Table 2
The wavelengths showed in them the maximum desalination by Z1 polysaccharide

Salt	λ (nm)	Salt removal percentage (%)
$CuSO_4$	415	89.74
$FeCl_3$	350	84.93
NH_4Cl[a]	410	73.4
Na_2SeO_3	350	7.38
$CoCl_2$	513	1.59

[a]After adding Nessler reagent.

3.7. FTIR analysis for interaction of different salts to Z1 polysaccharide

FTIR measurements were carried out to identify possible functional groups responsible for the reduction of different salts by Z1 polysaccharide. FTIR spectra peaks of polysaccharide and their assignments are shown in Table 3. In the comparison of FTIR spectra of polysaccharide itself with polysaccharide in each salt, there are some similarity and differences in the wave number and shape of the peaks. Different peaks are shown in Figs. 10–14 and Table 3.

3.7.1. $FeCl_3$

FTIR spectra peaks of polysaccharide in 0.3 mM $FeCl_3$ are shown in Table 3. As it is shown in Fig. 10, in the presence of $FeCl_3$, there is a shift from 3,305 to 3,362 cm⁻¹ that both of them represents the OH stretching in –COOH (carboxylic acids), and 2,854 cm⁻¹ is disappeared. Other differences are shown in the fingerprint region. There are some shifts: from 1,446 to 1,422 cm⁻¹, from 1,071 to 1,111 cm⁻¹, from 879 to 838 cm⁻¹, from 700 to 689 cm⁻¹ and from 536 to 481 cm⁻¹, and two peaks at 816 and 768 cm⁻¹ are disappeared. The most differences in presence of $FeCl_3$ are at the fingerprint region of spectra. But some of carboxyl groups (from 1,700 to 1,600 cm⁻¹) engaged in an Fe–carboxyl bond [47]. The strong peak at 1,655 cm⁻¹ that assignment C=O stretch (H-bond), shift to 1,653 cm⁻¹, suggesting a strong COO⁻–Fe(II or III) interaction.

Aryal and Liakopoulou-Kyriakides [48] used *Pseudomonas* sp. for biosorption of Fe(III) from wastewater. It could remove 86.206% of Fe(III) ions from solution. They showed that transmittance wave number in FTIR spectra at 3,370 and 1,380 cm⁻¹ shifted to 3,385 and 1,400 cm⁻¹ after Fe(III) absorption. It could be due to participation of the carboxylic and amine groups for interaction of Fe(III) ions by *Pseudomonas* sp. biomass surface. They believed that Fe(III) generally acts as a harder Lewis acid, since it can accept the lone pairs of electron, whereas amine group acts as a strong Lewis base due to the tendency to donate the lone pair of electron from N-atom, and this interaction of lone pair of electron from N-atom to Fe(III)-atom is considered to be stronger than electrostatic attractions (Fig. 11) [48].

In our experiment, transmittance wave number at 3,305 and 1,446 cm⁻¹ have been shifted to 3,362 and 1,422 cm⁻¹ after Fe(III) sorption, suggesting that the amine and carboxylic groups are mainly participated for Fe(III) ions interaction on Z1 polysaccharide.

Table 3
FTIR spectra peaks in interaction of Z1 polysaccharide with different salts

Z1 polysaccharide peaks (cm^{-1})	Structure	Assignment	P* + FeCl$_3$	P* + CuSO$_4$	P* + NH$_4$Cl	P* + Na$_2$SeO$_3$	P* + CoCl$_2$
			3,362				3,308
3,305	RCO–OH	Dimer OH		3,315	3,319	3,306	3,088
2,959	–CH$_3$	–CH$_3$	2,955	2,959	2,959	2,959	
2,927	–CH$_2$–	–CH$_2$–	2,927	2,928	2,927	2,926	2,928
2,874	–CH$_3$	–CH$_3$	2,874	2,871	2,874	2,874	2,871
2,854	–CH$_2$–	–CH$_2$–					
						1,728	
1,655	RCONHŔ	C=O stretch (H-bond)	1,653	1,652	1,658	1,655	1,644
1,539	N–O nitro comp	N–O asym. strech	1,546	1,542	1,537	1,540	1,542
1,446	C–C in ring	Ar C–C stretch			1,448	1,443	1,446
			1,422	1,412			1,416
1,386	S=O sulfate	S=O sulfate ester	1,388		1,386	1,383	1,392
				1,311			
1,237	RCO–OH	C–O stretch	1,223	1,226	1,235	1,230	1,229
			1,111	1,111			
1,071	RCO–OH	C–O stretch	1,065	1,066	1,069	1,058	1,072
				971			
879	1,2,4-trisub.	C–H out of plane	838		879		876
816	1,2,4-trisub.	C–H out of plane				827	
768	1,2,4-trisub.	C–H out of plane		778		768	775
700	Monosubst	C–H out of plan	689		698	700	
				625	621		622
536	R–Br	C–Br stretch	481		539	542	

P*: Z1 polysaccharide.
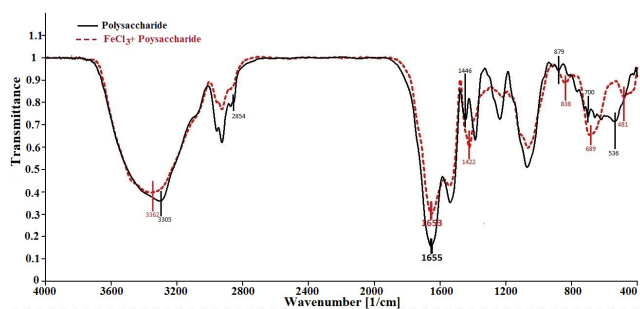

Fig. 10. Comparison of FTIR spectrum between polysaccharide and polysaccharide with FeCl$_3$.
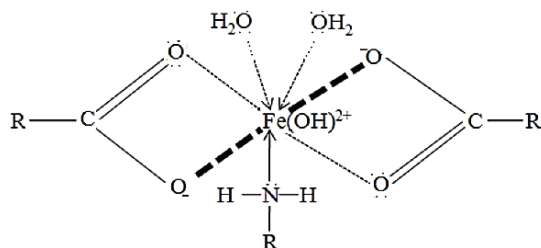

Fig. 11. Schematic possible interaction between Fe ion and biomass surface functional groups.
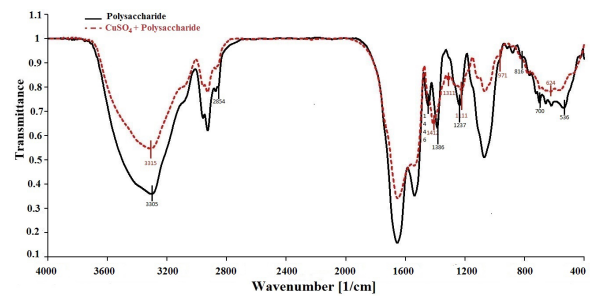

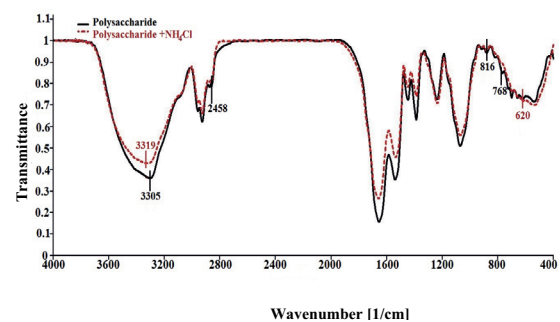Fig. 12. Comparison of FTIR spectrum between polysaccharide and polysaccharide with CuSO$_4$.

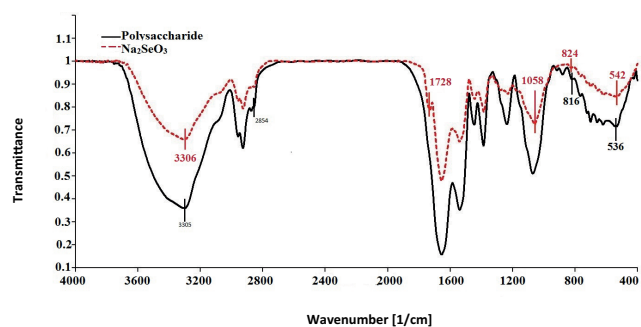Fig. 13. Comparison of FTIR spectrum between polysaccharide and polysaccharide with NH$_4$Cl.

Fig. 14. Comparison of FTIR spectrum between polysaccharide and polysaccharide with Na$_2$SeO$_3$.

3.7.2. CuSO$_4$

FTIR spectra peaks of polysaccharide in 1 mM CuSO$_4$ are shown in Table 3. CuSO$_4$ itself showed peaks at 1,627, 1,453, 1,345, 1,114, 988, 918, 851, 693, 582, 523 and 432 cm^{-1} [49]. Presence of the specific peaks at 1,311, 1,111 and 971 cm^{-1} in polysaccharide with 1 mM CuSO$_4$ is due to attachment of salt to polysaccharide. Comparison of FTIR spectrum between polysaccharide and polysaccharide with CuSO$_4$ is shown in Fig. 12.

As it is shown in Table 2, 89.74% of CuSO$_4$ was removed from solution by Z1 polysaccharide. It was shown that Cu(II) adsorption in two ways: ion exchanging in exchangeable cations and specific adsorption by a reaction between Cu(II) and functional surface groups [50].

3.7.3. NH$_4$Cl

FTIR spectra peaks of polysaccharide in 1 mM NH$_4$Cl are shown in Table 3. It was shown that NH$_4$Cl itself represent peaks at 3,150, 3,070, 2,860, 2,000, 1,780 and 1,410 cm^{-1} [49]. In the FTIR spectra, there is a shift from 3,305 to 3,319 cm^{-1} in presence of NH$_4$Cl that could be due to interaction between them (Fig. 13). It refers to N–H stretch band related to R$_2$NH structure of amines.

3.7.4. Na$_2$SeO$_3$

FTIR spectra peaks of polysaccharide in 1 mM Na$_2$SeO$_3$ are shown in Table 3. It was shown that Na$_2$SeO$_3$ represented peaks at 3,330, 1,450, 1,125, 788 and 730 cm^{-1} [49]. Therefore, presence of 1,728 cm^{-1} in polysaccharide with Na$_2$SeO$_3$ and the absence of it in polysaccharide itself spectra could be due to the interaction between Na$_2$SeO$_3$ and polysaccharide. These effects could be seen in their FTIR spectrum (Fig. 14).

3.7.5. CoCl$_2$

FTIR spectra peaks of polysaccharide in 0.4 mM CoCl$_2$ are shown in Table 3. However, it was shown that CoCl$_2$ itself represented peaks at 3,440, 3,393, 3,151, 1,620 and 781 cm^{-1} [51]. It can be concluded that presence of two peaks at 3,308 and 3,088 cm^{-1} in polysaccharide with CoCl$_2$ are due to the effect of CoCl$_2$. Differences that are observed at 1,200–700 cm^{-1} indicated that CoCl$_2$ can affected C–O–C and C–O groups, which dominated by ring vibrations in various

polysaccharide. FTIR spectra of polysaccharide and polysaccharide with CoCl$_2$ are shown in Fig. 15.

Bacillus atrophaeus is a gram-positive microorganism. Cell wall of gram-positive bacteria is made of peptidoglycan linked with teichoic acid and polysaccharides. Our isolated strain produced a large amount of exopolysaccharides due to its mucoidal colony. These structures possess functional groups such as carboxylic anions (COO$^-$), hydroxyl group (–OH), amine (–NH), and others, (–C–O), (–C=O), (–C–H), (–C–N–) that could adsorb different ions and molecules with different affinity [52]. Comparison of FTIR expectra of Z1-extracted polysaccharide with Z1 polysaccharides presence in different salt solution such as FeCl$_3$, CuSO$_4$, NH$_4$Cl, Na$_2$SeO$_3$ and CoCl$_2$ showed different picks resulted from interaction of functional groups with different ions. The results suggested that Z1 polysaccharide could be used as a biosorbent in water and wastewater treatment.

3.8. The effect of bacterial polymers and tragacanth on different elements and ions removal from well water

It was shown that when the same dry weight of tragacanth were added to the same volume of water or Z1 polysaccharide suspension, after 24 h, Z1 polysaccharide added to tragacanth was more swallowed than tragacanth by itself (Fig. 16). The atomic absorption results of the effects of these
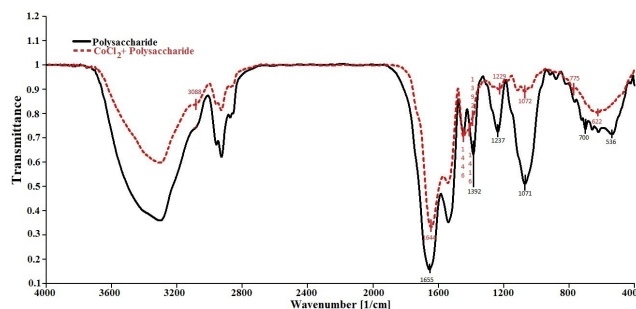

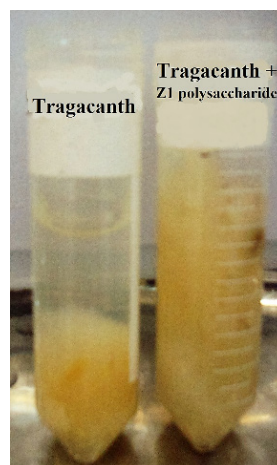Fig. 15. Comparison of FTIR spectrum between polysaccharide and polysaccharide with CoCl$_2$.

Fig. 16. Effect of tragacanth and Z1 polysacchride on biofilter construction.

Table 4
Atomic absorption results for the effect of tragacanth and Z1 polysaccharide biofilter on different ions removal

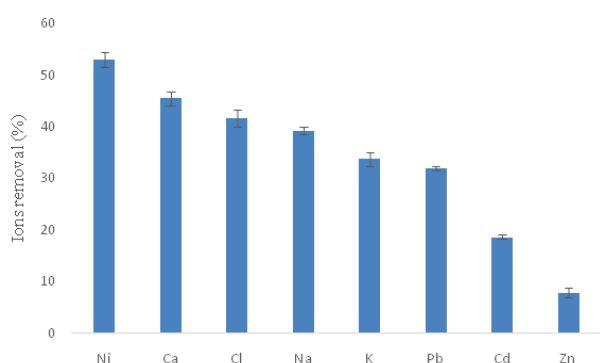|	Ca	K	Ni	Pb	Cd	Zn
Well water	1,140	10.6	0.2	0.2	0.016	0.05
Tragacanth	1,260	11.4	0.21	0.14	0.016	0.08
Z1 polysaccharide + tragacanth	1,360	14.6	0.19	0.23	0.026	0.12
Salt removal, (%)	43.33	33.64	53.66	32.35	18.75	7.69

Fig. 17. Ions removal percentage in the effluent of Z1 polysaccharide and tragacanth biofilter.

biofilters on different ions removal (Ca, K, Ni, Pb, Cd and Zn) showed that adding Z1 polysaccharide to tragacanth increased the ions deletion from well water (Table 4) and the most salt removal referred to Ni by 53.66%, and Zn removal was at least level between different metals by 7.69% (Fig. 17). The results of Na and Cl titration were added to atomic absorption results at Fig. 16.

Biosorption of copper (II) [20], chromium (VI) [22], lead [19], Ni(II) [17] and metal ions from aqueous solutions [21] were performed by different strains of *Bacillus* species.

4. Conclusion

A wide range of microorganisms such as bacteria, fungi, yeasts and algae are found in contaminated environments. Adsorption, oxidation, reduction, uptake and methylation are some of the mechanisms that they have developed to protect themselves against different salts and heavy metal toxicity [53]. The genus *Bacillus* has the important roles in the biotechnological application by producing antibiotics, exopolysaccharide, industrial enzymes and other commercial products. It was used as a biosorbent in water and wastewater treatments. Using bacterial polysaccharides instead of alive bacteria could prevent biofouling in biofilters. FTIR analysis of Z1 polysaccharide itself, and with different salts showed interaction of Z1 polysaccharide functional groups, such as –OH, –COO and C–O–C, involved in different ions and metal biosorption process. Participation of biopolymers such as tragacanth could improve biosorbent capacity of Z1 polysaccharide for different ions removal. Antimicrobial activity of Z1 polysaccharide adding to tragacanth in biofilter construction improved its properties for using them in water and wastewater desalination.

References

[1] K. Shubha, C. Raji, T. Anirudhan, Immobilization of heavy metals from aqueous solutions using polyacrylamide grafted hydrous tin (IV) oxide gel having carboxylate functional groups, Water Res., 35 (2001) 300–310.

[2] M.H. Habibi, M. Fakhrpor, Preparation of cerium zinc oxide nanocomposite derived by hydrothermal route coated on glass and its application in water treatment, Desal. Wat. Treat., 57 (2016) 26204–26210.

[3] X. Guo, Q. Wei, B. Du, Y. Zhang, X. Xin, L. Yan, H. Yu, Removal of basic dyes (malachite green) from aqueous medium by adsorption onto amino functionalized graphenes in batch mode, Desal. Wat. Treat., 53 (2015) 818–825.

[4] M. Sheibani, M. Ghaedi, F. Marahel, A. Ansari, Congo red removal using oxidized multiwalled carbon nanotubes: kinetic and isotherm study, Desal. Wat. Treat., 53 (2015) 844–852.

[5] F. Marahel, M.A. Khan, E. Marahel, I. Bayesti, S. Hosseini, Kinetics, thermodynamics, and isotherm studies for the adsorption of BR2 dye onto avocado integument, Desal. Wat. Treat., 53 (2015) 826–835.

[6] N.K. Singh, S. Saha, A. Pal, Solar light-induced photocatalytic degradation of methyl red in an aqueous suspension of commercial ZnO: a green approach, Desal. Wat. Treat., 53 (2015) 501–514.

[7] A. Rodríguez, J. García, G. Ovejero, M. Mestanza, Adsorption of anionic and cationic dyes on activated carbon from aqueous solutions: equilibrium and kinetics, J. Hazard. Mater., 172 (2009) 1311–1320.

[8] A. Bhatnagar, A. Jain, A comparative adsorption study with different industrial wastes as adsorbents for the removal of cationic dyes from water, J. Colloid Interface Sci., 281 (2005) 49–55.

[9] Q. Wang, W. Gao, Y. Liu, J. Yuan, Z. Xu, Q. Zeng, Y. Li, M. Schröder, Simultaneous adsorption of Cu(II) and SO_4^{2-} ions by a novel silica gel functionalized with a ditopic zwitterionic Schiff base ligand, Chem. Eng. J., 250 (2014) 55–65.

[10] F. Hashem, M. Amin, S. El-Gamal, Chemical activation of vermiculite to produce highly efficient material for Pb^{2+} and Cd^{2+} removal, Appl. Clay Sci., 115 (2015) 189–200.

[11] K.S. Shabani, F.D. Ardejani, K. Badii, M.E. Olya, Acid mine drainage treatment by perlite nanomineral, batch and continuous systems, Arch. Min. Sci., 59 (2014) 107–122.

[12] N. Karimi, M.A. Mohammadifar, Role of water soluble and water swellable fractions of gum tragacanth on stability and characteristic of model oil in water emulsion, Food Hydrocolloids, 37 (2014) 124–133.

[13] V. Kumar, P. Vikas, R. Kumar, B. Kumar, M. Kaur, Low cost natural polysaccharide and vinyl monomer based IPN for the removal of crude oil from water, J. Petrol. Sci. Eng., 141 (2016) 1–8.

[14] A. Yokoyama, K.R. Srinivasan, H.S. Fogler, Stabilization mechanism of colloidal suspensions by gum tragacanth: the influence of pH on stability, J. Colloid Interface Sci., 126 (1988) 141–149.

[15] S. Ghayempour, M. Montazer, M.M. Rad, Tragacanth gum as a natural polymeric wall for producing antimicrobial nanocapsules loaded with plant extract, Int. J. Biol. Macromol., 81 (2015) 514–520.

[16] M. Ranjbar-Mohammadi, S.H. Bahrami, M. Joghataei, Fabrication of novel nanofiber scaffolds from gum tragacanth/ poly (vinyl alcohol) for wound dressing application: in vitro evaluation and antibacterial properties, Mat. Sci. Eng., C, 33 (2013) 4935–4943.

[17] Y. Bulut, A. Gül, Z. Baysal, H. Alkan, Adsorption of Ni(II) from aqueous solution by Bacillus subtilis, Desal. Wat. Treat., 49 (2012) 74–80.

[18] Y. Göksungur, S. Üren, U. Güvenç, Biosorption of cadmium and lead ions by ethanol treated waste baker's yeast biomass, Bioresour. Technol., 96 (2005) 103–109.

[19] F. Çolak, N. Atar, D. Yazıcıoğlu, A. Olgun, Biosorption of lead from aqueous solutions by *Bacillus* strains possessing heavy-metal resistance, Chem. Eng. J., 173 (2011) 422–428.

[20] L.M. He, B.M. Tebo, Surface charge properties of and Cu (II) adsorption by spores of the marine *Bacillus* sp. strain SG-1, Appl. Environ. Microbiol., 64 (1998) 1123–1129.

[21] F. Masood, A. Malik, Biosorption of metal ions from aqueous solution and tannery effluent by Bacillus sp. FM1, J. Environ. Sci. Health., Part A, 46 (2011) 1667–1674.

[22] Y. Şahin, A. Öztürk, Biosorption of chromium(VI) ions from aqueous solution by the bacterium *Bacillus thuringiensis*, Process Biochem., 40 (2005) 1895–1901.

[23] M. Sára, D. Pum, U. Sleytr, Permeability and charge-dependent adsorption properties of the S-layer lattice from Bacillus coagulans E38-66, J. Bacteriol., 174 (1992) 3487–3493.

[24] X. Zhou, X. Jiao, Polymerase chain reaction detection of *Listeria monocytogenes* using oligonucleotide primers targeting *actA* gene, Food Control, 16 (2005) 125–130.

[25] O.-S. Kim, Y.-J. Cho, K. Lee, S.-H. Yoon, M. Kim, H. Na, S.-C. Park, Y.S. Jeon, J.-H. Lee, H. Yi, Introducing EzTaxon-e: a prokaryotic 16S rRNA gene sequence database with phylotypes that represent uncultured species, Int. J. Syst. Evol. Microbiol., 62 (2012) 716–721.

[26] K. Tamura, G. Stecher, D. Peterson, A. Filipski, S. Kumar, MEGA6: molecular evolutionary genetics analysis version 6.0, Mol. Biol. Evol., 30 (2013) 2725–2729.

[27] N. Gholampoor, G. Emtiazi, Z. Emami, The influence of Microbacterium hominis and Bacillus licheniformis extracellular polymers on silver and iron oxide nanoparticles production; green biosynthesis and mechanism of bacterial nano production, J. Nanomater. Mol. Nanotechnol., 6 (2015) 1–6.

[28] D. Stafford, The effect of phenols and heterocyclic bases on nitrification in activated sludges, J. Appl. Bacteriol., 37 (1974) 75–82.

[29] L. Nakamura, Taxonomic relationship of black-pigmented *Bacillus subtilis* strains and a proposal for *Bacillus atrophaeus* sp. nov., Int. J. Syst. Evol. Microbiol., 39 (1989) 295–300.

[30] S.R. Sella, L.P. Vandenberghe, C.R. Soccol, Bacillus atrophaeus: main characteristics and biotechnological applications–a review, Crit. Rev. Biotechnol., 35 (2015) 533–545.

[31] R. Davis, L. Mauer, Fourier Transform Infrared (FT-IR) Spectroscopy: A Rapid Tool for Detection and Analysis of Foodborne Pathogenic Bacteria, Current Research, Technology and Education Topics in Applied Microbiology and Microbial Biotechnology, Vol. 2, 2010, pp. 1582–1594.

[32] S. Raveendran, B. Dhandayuthapani, Y. Nagaoka, Y. Yoshida, T. Maekawa, D.S. Kumar, Biocompatible nanofibers based on extremophilic bacterial polysaccharide, Mauran from *Halomonas maura*, Carbohydr. Polym., 92 (2013) 1225–1233.

[33] C.A. Tischer, M. Iacomini, P.A.J. Gorin, Structure of the arab-inogalactan from gum tragacanth (Astralagus gummifer), Carbohydr. Polym., 337 (2002) 1647–1655.

[34] M.J. Zohuriaan, F. Shokrolahi, Thermal studies on natural and modified gums, Polym. Test., 23 (2004) 575–579.

[35] F. Chenlo, R. Moreira, C. Silva, Rheological behaviour of aqueous systems of tragacanth and guar gums with storage time, J. Food Eng., 96 (2010) 107–113.

[36] S.J.J. Debon, R.F. Tester, In vitro binding of calcium, iron and zinc by non-starch polysaccharides, Food Chem., 73 (2001) 401–410.

[37] M. Farzi, M.S. Yarmand, M. Safari, Z. Emam-Djomeh, M.A. Mohammadifar, Gum tragacanth dispersions: particle size and rheological properties affected by high-shear homogenization, Int. J. Biol. Macromol., 79 (2015) 433–439.

[38] L.C.M. Das Neves, K.S. De Oliveira, M.J. Kobayashi, T.C.V. Penna, A. Converti, Biosurfactant production by cultivation of Bacillus atrophaeus ATCC 9372 in semidefined glucose/casein-based media, Appl. Biochem. Biotechnol., 137–140 (2007) 539–554.

[39] S.S. Shelar, S.S. Warang, S.P. Mane, R.L. Sutar, J.S. Ghosh, Characterization of bacteriocin produced by Bacillus atrophaeus strain JS-2, Int. J. Biol. Chem., 6 (2012) 10–16.

[40] X. Zhang, B. Li, Y. Wang, Q. Guo, X. Lu, S. Li, P. Ma, Lipopeptides, a novel protein, and volatile compounds contribute to the antifungal activity of the biocontrol agent Bacillus atrophaeus CAB-1, Appl. Microbiol. Biotechnol., 97 (2013) 9525–9534.

[41] A. Matin, Z. Khan, S. Zaidi, M. Boyce, Biofouling in reverse osmosis membranes for seawater desalination: phenomena and prevention, Desalination, 281 (2011) 1–16.

[42] T. Stein, S. Düsterhus, A. Stroh, K.-D. Entian, Subtilosin production by two *Bacillus subtilis* subspecies and variance of the *sbo-alb* cluster, Appl. Environ. Microbiol., 70 (2004) 2349–2353.

[43] F. Liu, W. Sun, F. Su, K. Zhou, Z. Li, Draft genome sequence of the sponge-associated strain *Bacillus atrophaeus* C89, a potential producer of marine drugs, J. Bacteriol., 194 (2012) 4454–4454.

[44] J. Hill, Silica gel as an insoluble carrier for the preparation of selective chromatographic adsorbents: the preparation of 8-hydroxyquinonline substituted silica gel for the chelation chromatography of some trace metals, J. Chromatogr., A, 76 (1973) 455–458.

[45] X. Yu, C. Wei, H. Wu, Effect of molecular structure on the adsorption behavior of cationic dyes onto natural vermiculite, Sep. Purif. Technol., 156 (2015) 489–495.

[46] N. Sakairi, S. Suzuki, K. Ueno, S.-M. Han, N. Nishi, S. Tokura, Biosynthesis of hetero-polysaccharides by *Acetobacter xylinum*-synthesis and characterization of metal-ion adsorptive properties of partially carboxymethylated cellulose, Carbohydr. Polym., 37 (1998) 409–414.

[47] P. Calvini, M. Silveira, FTIR analysis of naturally aged $FeCl_3$ and $CuCl_2$-doped cellulose papers, e-Preserv.Sci., 5 (2008) 1–6.

[48] M. Aryal, M. Liakopoulou-Kyriakides, Binding mechanism and biosorption characteristics of Fe(III) by Pseudomonas sp. cells, J. Water Sustainability, 3 (2013) 117–131.

[49] F.A. Miller, C.H. Wilkins, Infrared spectra and characteristic frequencies of inorganic ions, Anal. Chem., 24 (1952) 1253–1294.

[50] E. Eren, B. Afsin, An investigation of Cu(II) adsorption by raw and acid-activated bentonite: a combined potentiometric, thermodynamic, XRD, IR, DTA study, J. Hazard. Mater., 151 (2008) 682–691.

[51] I. Gamo, Infrared spectra of water of crystallization in some inorganic chlorides and sulfates, Bull. Chem. Soc. Jpn., 34 (1961) 760–764.

[52] A. Ayla, A. Çavuş, Y. Bulut, Z. Baysal, C. Aytekin, Removal of methylene blue from aqueous solutions onto *Bacillus subtilis*: determination of kinetic and equilibrium parameters, Desal. Wat. Treat., 51 (2013) 7596–7603.

[53] A. Zahoor, A. Rehman, Isolation of Cr(VI) reducing bacteria from industrial effluents and their potential use in bioremediation of chromium containing wastewater, J. Environ. Sci., 21 (2009) 814–820.